REPORT DOCUMENTATION PAGE

Form Approved
OMB No. 0704-0188

PLEASE DO NOT RETURN YOUR FORM TO THE ABOVE ORGANIZATION.

1. REPORT DATE *(DD-MM-YYYY)*	2. REPORT TYPE	3. DATES COVERED *(From - To)*
11-05-2015	Conference Proceedings	

4. TITLE AND SUBTITLE

A miniature fiber-optic sensor for high-resolution and high-speed temperature sensing in ocean environment

5a. CONTRACT NUMBER

5b. GRANT NUMBER

5c. PROGRAM ELEMENT NUMBER

0602435N

6. AUTHOR(S)

Guigen Liu, Ming Han, Weilin Hou, Silvia Matt, and Wesley Goode

5d. PROJECT NUMBER

5e. TASK NUMBER

5f. WORK UNIT NUMBER

73-4951-05-5

7. PERFORMING ORGANIZATION NAME(S) AND ADDRESS(ES)

Naval Research Laboratory
Oceanography Division
Stennis Space Center, MS 39529-5004

8. PERFORMING ORGANIZATION REPORT NUMBER

NRL/PP/7330--15-2536

9. SPONSORING/MONITORING AGENCY NAME(S) AND ADDRESS(ES)

Office of Naval Research
One Liberty Center
875 North Randolph Street, Suite 1425
Arlington, VA 22203-1995

10. SPONSOR/MONITOR'S ACRONYM(S)

ONR

11. SPONSOR/MONITOR'S REPORT NUMBER(S)

12. DISTRIBUTION/AVAILABILITY STATEMENT

Approved for public release, distribution is unlimited.

13. SUPPLEMENTARY NOTES

14. ABSTRACT

Temperature measurement is one of the key quantifies in ocean research. Temperature variations on small and large scales are key to air-sea interactions and climate change, and also regulate circulation patterns, and heat exchange. The influence from rapid temperature changes within microstructures are can have strong impacts to optical and acoustical sensor performance. In this paper, we present an optical fiber sensor for the high-resolution and high-speed temperature profiling. The developed sensor consists of a thin piece of silicon wafer which forms a Fabry-Pérot interferometer (FPI) on the end of fiber. Due to the unique properties of silicon, such as large thermal diffusivity, notable thermo-optic effects and thermal expansion coefficients of silicon, the proposed sensor exhibits excellent sensitivity and fast response to temperature variation. The small mass of the tiny probe also contributes to a fast response due to the large surface-tovolume ratio. The high reflective index at infrared wavelength range and surface flatness of silicon endow the FPI a spectrum with high visibilities, leading to a superior temperature resolution along with a new data processing method developed by us. Experimental results indicate that the fiber-optic temperature sensor can achieve a temperature resolution better than 0.001°C with a sampling frequency as high as 2 kHz. In addition, the miniature footprint of the senor provide high spatial resolutions. Using this high performance thermometer, excellent characterization of the realtime temperature profile within the flow of water turbulence has been realized.

15. SUBJECT TERMS

Fiber-optic sensors, Fabry-Pérot interferometer, thermometer, high-speed detection

16. SECURITY CLASSIFICATION OF:			17. LIMITATION OF ABSTRACT	18. NUMBER OF PAGES	19a. NAME OF RESPONSIBLE PERSON
a. REPORT	b. ABSTRACT	c. THIS PAGE			Weilin Hou
Unclassified	Unclassified	Unclassified	UU	6	19b. TELEPHONE NUMBER *(Include area code)* (228) 688-5257

Reset

15-1231-1321

PUBLICATION OR PRESENTATION RELEASE REQUEST

Pubkey 9[illegible]9 NRLINST 5510.40

1. REFERENCES AND ENCLOSURES	2. TYPE OF PUBLICATION OR PRESENTATION		3. ADMINISTRATIVE INFORMATION
Ref: (a) NRL Instruction 5600.2 (b) NRL Instruction 5510.40E Encl: (1) Two copies of subject publication/presentation	( ) Abstract only, published	( ) Abstract only, not published	STRN NRL/PP/7330-15-2535 Route Sheet No. 7330/ Job Order No. 73-4951-05-5 Classification U S C FOUO Sponsor ONR BASE 6.1 Bay Sponsor's approval yes (attached) (*Required if research is other than 6.1/6.2 NRL or ONR unclassified research or if publication/presentation is classified
	( ) Book author	( ) Book chapter	
	( ) Book editor	( ) Multimedia report	
	(X) Conference Proceedings (refereed)	( ) Conference Proceedings (not refereed)	
	( ) Journal article (refereed)	( ) Journal article (not refereed)	
	( ) Oral Presentation, published	( ) Oral Presentation, not published	
	( ) Video ( ) Poster	( ) Other, explain	
	ALL DOCUMENTS/PRESENTATIONS MUST BE ATTACHE		

4. AUTHOR

Title of Paper or Presentation

A miniature fiber-optic sensor for high-resolution and high-speed temperature and flow sensing in ocean environment

AUTHOR(s) LEGAL NAMES(s) OF RECORD (First, MI, Last), CODE, (Affiliation if not NRL).

Guigen Liu University of Nebraska-Lincoln, Weilin Hou 7333, Silvia Matt 7333, Wesley A. Goode 7333, Ming Han University of Nebraka-Lincoln,

This paper will be presented at the OSA Imaging and Applied Optics Meeting
(Name of Conference)

07-JUN - 11-JUN-15, Arlington, VA, Unclassified
(Date, Place and Classification of Conference)

and/or for published in OSA Imaging and Applied Optics Meeting, Unclassified
(Name and Classification of Publication) (Name of Publisher)

5. CERTIFICATION OR CLASSIFICATION

It is my opinion that the subject paper (is ____) (is not __x__) classified, in accordance with reference (b) and this paper does not violate any disclosure of trade secrets or suggestions of outside individuals or concerns which have been communicated to the NRL in confidence.

This subject paper (has ____) (has never __x__) been incorporated in an official NRL Report.

Weilin Hou, 7333 — Weilin Hou
Name and Code (Principal Author) (Legal Name of Record and Signature Only) (Signature)

6. ROUTING/APPROVAL (NOTE: If name other than your legal name of record is annotated on the publication or presentation itself, add an explanatory note in the "comments" section below next to your signed legal name of record)

CODE	SIGNATURE	DATE	COMMENTS
Co-Author(s) Weilin Hou, 7333	Weilin Hou	4/8/15	Need by 29 Apr 2015
			This is a Final Security Review. Any changes made in the document, after approved by Code 1231, nullify the Security Review.
Section Head			
Branch Head Richard L. Crout, 7330	Richard L. Crout	4-8-2015	
Division Head Ruth H. Preller, 7300	Ruth H. Preller	4/9/15	1. To the best knowledge of this Division, the subject matter of this publication (has ____)(has never ____ X)been classified. 2. This paper (does ____) (does not __X__) contain any militarily critical technology.
ADOR/Director NCST E. R. Franchi, 7000			
~~SO/USO~~			
Security, Code 1231	Susan	4/20/15	A copy of the paper, abstract or presentation is filed in this office.
Associate Counsel Code 1008.3	recede invention memo 5/7/15		
Public Affairs (Unclassified/Unlimited Only), Code 7030.4	Shannon Mensi	4-27-15	
Division, Code			
Author, Code			

HQ-NRL 5511/6 (Rev. 12/14) THIS FORM CANCELS AND SUPERSEDES ALL PREVIOUS VERSIONS

15 APR 15 10:25

A miniature fiber-optic sensor for high-resolution and high-speed temperature sensing in ocean environment

Guigen Liu[1], Ming Han[1,*] Weilin Hou[2], Silvia Matt[2], and Wesley Goode[2]
[1]Department of Electrical Engineering, University of Nebraska-Lincoln, Lincoln, NE 68588, USA
[2]Naval Research Laboratory, Code 7333, Stennis Space Center, MS 39529, USA
* Corresponding author: mhan3@unl.edu

ABSTRACT

Temperature measurement is one of the key quantifies in ocean research. Temperature variations on small and large scales are key to air-sea interactions and climate change, and also regulate circulation patterns, and heat exchange. The influence from rapid temperature changes within microstructures are can have strong impacts to optical and acoustical sensor performance. In this paper, we present an optical fiber sensor for the high-resolution and high-speed temperature profiling. The developed sensor consists of a thin piece of silicon wafer which forms a Fabry-Pérot interferometer (FPI) on the end of fiber. Due to the unique properties of silicon, such as large thermal diffusivity, notable thermo-optic effects and thermal expansion coefficients of silicon, the proposed sensor exhibits excellent sensitivity and fast response to temperature variation. The small mass of the tiny probe also contributes to a fast response due to the large surface-to-volume ratio. The high reflective index at infrared wavelength range and surface flatness of silicon endow the FPI a spectrum with high visibilities, leading to a superior temperature resolution along with a new data processing method developed by us. Experimental results indicate that the fiber-optic temperature sensor can achieve a temperature resolution better than 0.001°C with a sampling frequency as high as 2 kHz. In addition, the miniature footprint of the senor provide high spatial resolutions. Using this high performance thermometer, excellent characterization of the real-time temperature profile within the flow of water turbulence has been realized.

Keywords: Fiber-optic sensors, Fabry-Pérot interferometer, thermometer, high-speed detection.

1. INTRODUCTION

Temperature measurement is an important aspect of oceanography, which functions as a key step toward field application in both civilian and military environment [1, 2]. Currents, mixing events, large-scale circulation, air-sea exchange, and certainly global climate change are a few obvious examples. Temperature fluctuations, especially on the small scale, also affects sensor and system performance. For example, diver visibility, search and rescue at sea, mine detection all rely on the underwater imaging capability. It has been shown recently, that not only the turbidity affects image quality, but also optical turbulence. As we know, turbidity is caused by particle absorption but mostly scattering in the water. It thus may be inferred that this issue does not exist in clean waters like clean lakes and rivers. But in reality, another factor, i.e., the optical turbulence, can take over and play the dominant role in determining the imaging quality in these clear waters [3], and can also affect acoustical signal propagation [4].

While salinity variations could sometimes lead to severe turbulence [5], temperature gradient is the primary contributing element that triggers the underwater optical turbulence by modifying the index of refraction within the microstructures. To better understand the process, and possibly to facilitate rectification of the image blurred by the turbulence, a full characterization of the temperature distribution at the highest sampling rate and at the smallest spatial scale is critical. Specifically, it's reported that a sensor with singe-pole time constant less than and spatial resolution better than is required to estimate the rate of dissipation of temperature variance in turbulent heat flux model [6]. To tackle the issue regarding the fast and high-resolution measurement of localized temperature, several efforts have been made by resort to a tiny thermistor or thermocouple [6, 7]. However, interferences from the environment, such as strong electromagnetic field from lightening, erroneous signals or corrosion from strong salinity, etc., prevent the thermocouples from being reliable sensors. Furthermore, the long-distance transmission of the weak electronic signals is a big challenge.

In this paper, we will study an alternative high-resolution and fast-response fiber-optic temperature sensor we recently developed [8]. It consists of a tiny silicon cylinder assembled on the endface of a single-mode fiber (SMF). The silicon cylinder serves as a Fabry-Pérot interferometer (FPI) which sends back an interferometric spectrum that is

Ocean Sensing and Monitoring VII, edited by Weilin W. Hou, Robert A. Arnone, Proc. of SPIE Vol. 9459
94590I · © 2015 SPIE · CCC code: 0277-786X/15/$18 · doi: 10.1117/12.2180168

sensitive to the silicon temperature. Due to the large thermo-optic coefficient of silicon, the investigated sensor has a high temperature sensitivity. To increase the temperature resolution by reducing noise, an average wavelength tracking previously developed by us will be applied [8]. The small size of the sensing silicon, no longer than 200 μm and no thicker than 100 μm, endows the sensor with miniature footprint which is a big advantage for surveillance of temperature variation at a tiny spot. With such small size, along with the high thermal diffusivity of silicon, the fiber sensor features swift response to follow the fast temperature variation within the turbulence. Furthermore, the extremely small optical attenuation (0.1 dB/km) within the SMF is superior when it comes to remote sensing in far and deep ocean. As an initial test, the real-time temperature structure within the water microstructure generated by two methods will be demonstrated. Comparison in performance of the investigated sensor with the mostly used commercial high-speed thermistor FP07 (GE Thermometrics) will also be provided.

2. PRINCIPLE AND THEORY

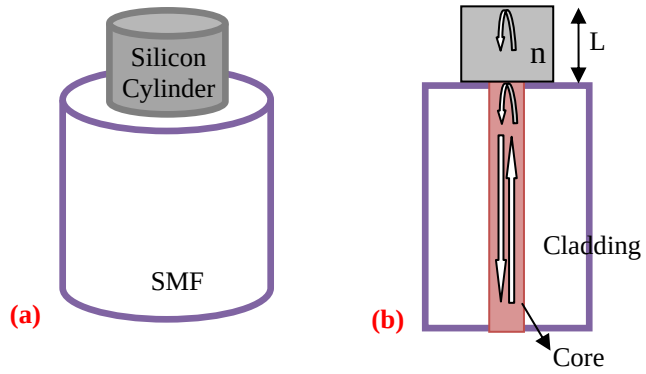

Figure 1. (a) Schematic structure of the sensor head and (b) illustration of the principle of operation.

Structure of the sensor head is shown in Fig. 1(a). According to the procedure described in detail in our previous report [8], the cylindrical silicon can be mounted on the cleaved endface of a SMF. The silicon cylinder works as a Fabry-Pérot interferometer (FPI), as shown in Fig. 1(b). Two reflections at the fiber-silicon and silicon-surrounding interfaces combine and send back an interferometric spectrum which features a series of dip and peak wavelengths. If refractive index of the silicon material is defined as n and length of the cylinder is denoted as L, then the optical path difference (OPT) between these two reflected lights will determine the Nth peak wavelength, λ_N, following this formula below

$$\left(N+\frac{1}{2}\right)\lambda_N = 2nL\,. \tag{1}$$

The inherent properties, i.e., thermo-optic effect and thermal expansion, give birth to the temperature dependence of both n and L in Eq. (1). Consequently, the peak wavelength λ_N is a function of temperature, which is explored to monitor the environmental temperature variation. Temperature sensitivity, k, of the peak wavelength derived from Eq. (1) can be expressed as

$$k = \frac{\partial \lambda_N}{\partial T} = \lambda_N \left(\frac{1}{n}\frac{\partial n}{\partial T} + \frac{1}{L}\frac{\partial L}{\partial T}\right). \tag{2}$$

Right-hand side (RHS) of Eq. (2) includes two parts, one is the contribution of thermo-optic effects, $k_{TO} = \lambda_N \frac{1}{n}\frac{\partial n}{\partial T}$; the other part is contribution of thermal expansion, $k_{TE} = \lambda_N \frac{1}{L}\frac{\partial L}{\partial T}$. As an estimation, $k_{TO} = 68.4\,pm/℃$ and $k_{TE} = 4\,pm/℃$ are obtained using the thermo-optic coefficient (TOC) of $1.5\times10^{-4}\,RIU/℃$ and thermal expansion coefficient (TEC) of $2.55\times10^{-6}\,m/(m\cdot℃)$ at temperature of 25 ℃, evaluated around $1550\,nm$ and $n = 3.4$ for silicon. It's clear that the total sensitivity of $k = k_{TO} + k_{TE} = 72.4\,pm/℃$ is mainly attributed to the thermo-optic effects.

To predict the speed of this sensor in response to temperature change, a heat transfer analysis should be performed. As our previous work has provided theoretical analysis on this issue [8], a brief reproduction of the theory is extracted here to facilitate interpretation and evaluation of the sensor response time with extended detailed analysis on the influence of sensor size on the response time. Due to the high thermal conductivity and small thermal mass, whenever there is a thermal exchange between the sensor head and surrounding, the heat energy dissipates so fast within the silicon

cylinder that the temperature gradient is ignorable. In such a situation, the formula for heat transfer analysis is reduced to the following lamped parameter model [9]

$$hA_s(T_\infty - T)dt = \rho_s C_s V_s dT\,, \tag{3}$$

where T_∞ and T are, respectively, the steady-state and transient temperature of silicon cylinder; A_s is the surface area through which heat exchanges; ρ_s, C_s, and V_s are, respectively, mass density, heat capacity and volume of the silicon FPI; h is the heat transfer coefficient. Solution to Eq. (3) is given as

$$T(t) = T_\infty + (T_0 - T_\infty)\exp\left(-\frac{hA_s}{\rho_s C_s V_s}t\right), \tag{4}$$

where T_0 is the initial temperature of the silicon sensor head. Thus, combination of Eqs. (2) and (4) produces the following temperature-dependent peak wavelength

$$\lambda(t) = \lambda_0 + kT_\infty + k(T_0 - T_\infty)\exp\left(-\frac{hA_s}{\rho_s C_s V_s}t\right), \tag{5}$$

where λ_0 is the intercept wavelength. Obviously, the RHS of Eq. (5) includes a transient item, from which the response time, defined as the time needed when the signal rises to 1/e of the total change, is extracted as follows

$$\tau = \frac{\rho_s C_s V_s}{hA_s}\,. \tag{6}$$

To obtain the value of response time τ, it's necessary to first get the value of heat transfer coefficient h. Using the Nusselt number N_u and heat conductivity K_w of water, h can be calculated as [9]

$$h = \frac{N_u \cdot K_w}{L_c}\,. \tag{7}$$

where $L_c = V_s/A_s$ is the characteristic length. Substituting Eq. (7) into Eq. (6) and taking $A_s = \pi DL + \pi D^2/4$ and $V_s = \pi D^2 L/4$, where D and L are, respectively, diameter and length of the silicon cylinder, give rise to

$$\tau = \frac{\rho_s C_s}{N_u K_w}\frac{L^2 D^2}{(4L + D)^2}\,. \tag{8}$$

Eq. (8) gives an explicit dependence of response time on the size of the silicon cylinder.

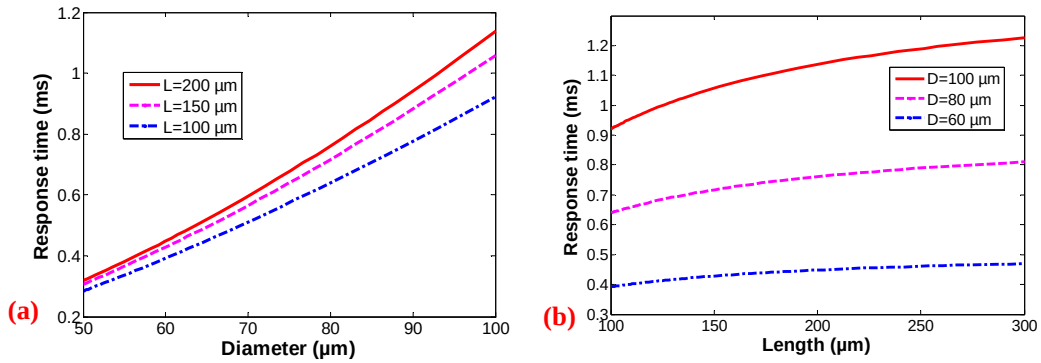

Figure 2. Calculated response time as a function of (a) diameter and (b) length of the cylindrical silicon FPI.

Taking $N_u = 1.2$ for the heat transfer on the water/silicon surface [10], $K_w = 0.6\,W/(m \cdot K)$, $C_s = 712\,\mathrm{J/(kg \cdot K)}$, and $\rho_s = 2.329 \times 10^3\,\mathrm{kg/m^3}$, the calculated response time versus diameter and length of silicon cylinder is shown in Fig. 2. It can be inferred from Fig. 2(a) that by reducing diameter of the silicon cylinder the response time decreases. Also, by reducing length of the silicon cylinder the response time decreases, as illustrated in Fig. 2(b). If diameter and length of the silicon pillar are, respectively, 50 μm and 100 μm, then a response time as short as ~0.3 ms is evaluated. The reduced size (diameter and length) of the sensing silicon facilitates the heat exchange between the sensor head and environment, therefore, it is more favorable if reduced sensing mass is applied. However, the reduced size of the sensor head will extremely increase the difficulty of the assembling procedure depicted in detail in [8]. Furthermore, the divergent outgoing rays from the single-mode fiber may expand out of the silicon pillar if its diameter is too small, leading to a degraded visibility and thus limited temperature resolution. Lastly, we have demonstrated in [8] that an average wavelength tracking method taking advantage of the dense fringes will help reduce noise, but a reduced length

of the silicon cylinder is a contradiction to this advantage, because a reduced length results in a larger free spectral range and consequently fewer peaks used for calculating the average wavelength. Therefore, a balance between response time and resolution should be considered while choosing the size of the sensing element.

3. EXPERIMENTATION

3.1 Temperature resolution and response time

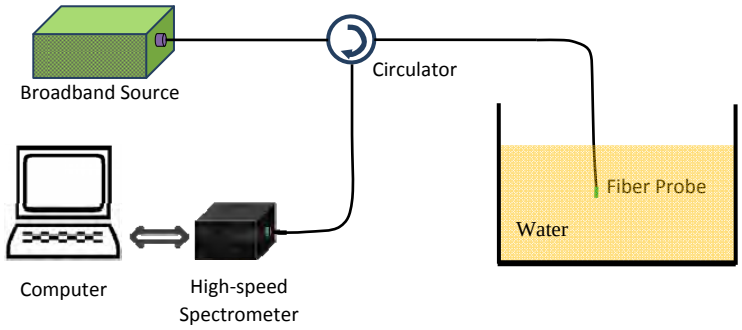

Figure 3. Experimental setup

Experimental demonstration of the sensor performance has been carried out using the setup exhibited in Fig. 3. The broadband source provides the wide-band spectrum for average wavelength tracking. The high-speed spectrometer (I-MON 256, Ibsen Photonics) with a maximum sampling frequency of 6 kHz guarantees the swift capture of spectrum variation over time.

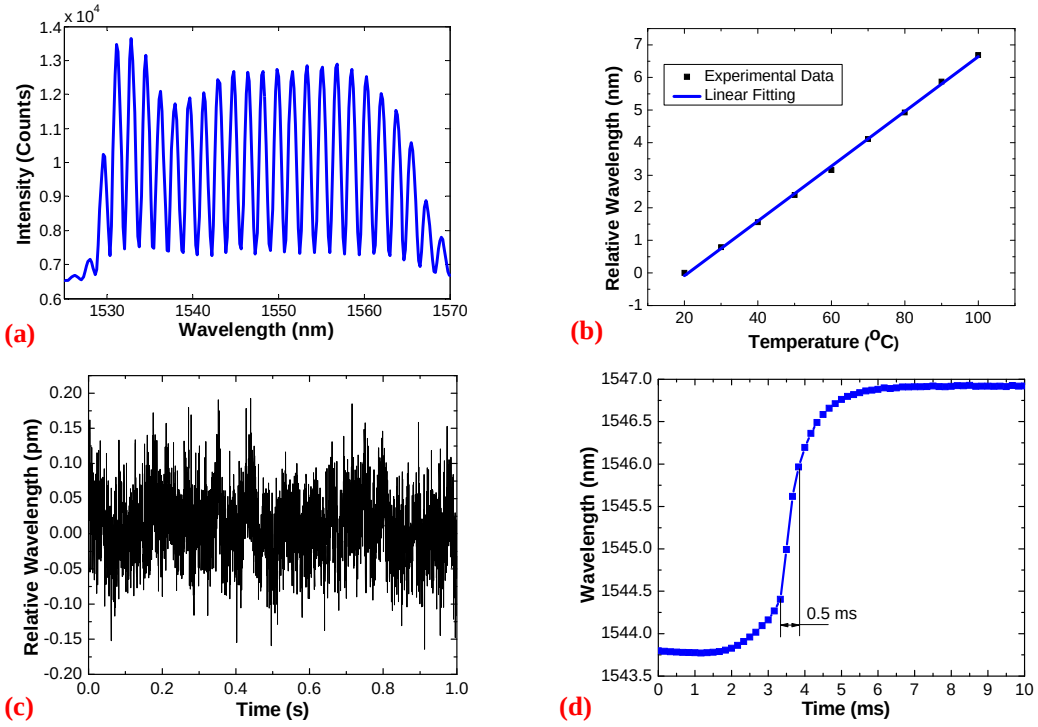

Figure 4. (a) A typical reflection spectrum obtained from the sensor. (b) Relative wavelength shift as a function of temperature. (c) Wavelength noise versus time. (d) Temporal wavelength while dipping the sensor head from air (~20 ℃) into hot water (~58 ℃).

One typical frame of the spectrum is shown in Fig. 4(a), from which dozens of fringe peaks are inspected, owing to the small free spectrum range of only 1.726 nm. To make full use of the large amount of peaks, we have proposed and investigated an average wavelength tracking method to reduce the noise [8], which is also applied in this paper. In the experimental results shown in Fig. 4, we used 22 peaks that were centered around 1545 nm. The temperature sensitivity was first measured and the results are shown in Fig. 4(b). An excellent linear response was observed within the temperature range of 20-100 ℃, indicating a temperature sensitivity of 84 pm/℃. By immersing the sensor into the water stabilized in the room temperature (around 22 ℃) and recording the spectrum for one second with a sampling frequency of 6 kHz and integration time of 100 μs, the wavelength noise was characterized and the results are shown in Fig. 4(c). The standard deviation of ~0.0504 pm of the wavelength variation during this period is defined as the noise level, leading to a temperature resolution of 6×10^{-4} ℃. The high resolution guarantees the visualization of subtle variation in the local water. To test the response time of the proposed sensor, the sensor head was fast dipped into a cup of hot water. The temporal variation in wavelength is shown in Fig. 4(d), from which it can be seen that the fast response of the sensor started to show up before it hit the water at the time of around 3.5 ms, which was due to the warmed up air and water vapor. After that a sharp increase in the wavelength was observed upon immersing in the hot water. From the curve in Fig. 4(d), a response time of 0.5 ms is inferred, suggesting a sampling frequency as high as 2 kHz can be achieved.

3.2 Flow sensing in water turbulence

To demonstrate the performance of the investigated sensor in profiling the temperature variation within water turbulence, two experiments were carried out. In the first experiment, the turbulence was created by putting an icebag on the surface of water. The water cooled down by the icebag went down quickly and in the meantime warm water rose, thus creating a turbulence and leading to the variation in temperature at the fixed point where the fiber sensor was placed. The whole process was perfectly monitored by our fiber thermometer, as shown by Fig. 5(a).

In the second experiment, the turbulence was generated by pouring some hot water into a bucket of cool water. This time, the fiber sensor was compared with a commercial fast-response thermistor (FP07) which served both as a reference and as a calibration. The two sensors were deployed in the vicinity of each other. Comparison between these two sensors is shown in Fig. 5(b). Apparently, the fiber sensor followed the FP07 thermistor very well but tracked much more details of the swift temperature alteration. These useful temperature profile will provide a powerful tool for the analysis of influence of underwater turbulence on imaging in the ocean. Data were also collected in a simulated turbulence environment, utilizing a Rayleigh-Benard convective tank. More details can be found in a companion paper by Matt et al. [11].

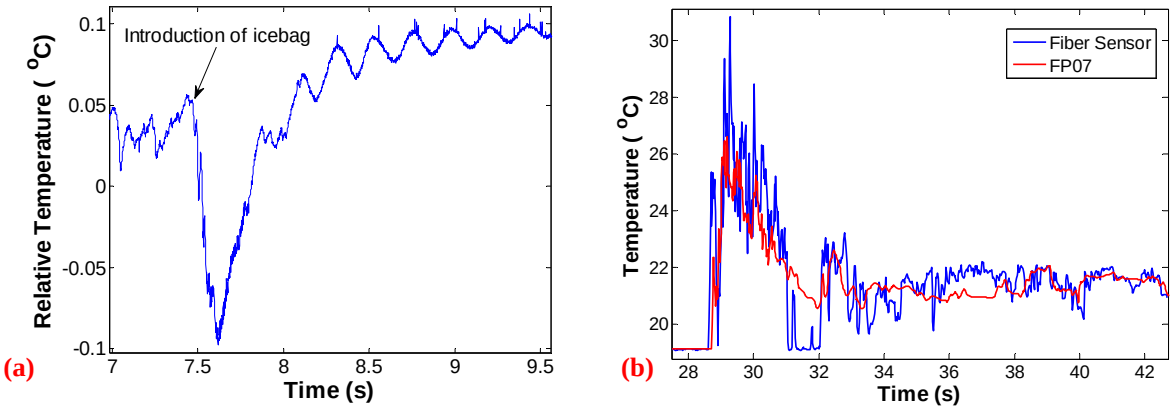

Figure 5. Detection of water turbulence generated by (a) putting an ice bag on the surface of water and (b) pouring some hot water into a bucket of cool water. In (b), response of the commercial high-speed thermistor FP07 is provided as calibration and reference.

4. CONCLUSION

In summary, this work describes a novel fiber-optic thermometer that features high temperature resolution and fast response for the oceanographic applications. Theoretical investigation suggests that an increase in sampling rate can be

obtained by reducing the size (diameter or length) of the silicon cylinder. For example, a 50-μm-diameter and 100-μm-length silicon pillar is theoretically predicted to possess a response time as low as 0.3 ms. In experiments, a sensor with 80-μm-diameter and 200-μm-length silicon pillar was capable of resolving a temperature variation as low as 6×10^{-4} ℃ and sampling at a frequency as high as 2 kHz. Using this sensor, temperature variation within turbulence microstructure has been successfully tracked. The water turbulence was initiated by two ways, one is floating an icebag on the water, and the other is pouring some hot water into a bucket of cool water. Outperformance of the proposed fiber sensor over a commercial high-speed thermistor FP07 in characterizing the temperature fluctuation within the turbulence manifests this powerful tool, which exhibits a great promise for applications in oceanography.

5. ACKNOWLEDGMENT

This work was partially supported by the U.S. Naval Research Laboratory under grant no. N0017315P0376.

6. REFERENCE

[1] W. Hou, *Ocean sensing and monitoring* (SPIE Press, 2013).
[2] J. S. Jaffe, "Underwater optical imaging: the past, the present, and the prospects," IEEE J. Oceanic Eng., in press
[3] W. Hou, S. Woods, E. Jarosz, W. Goode, and A. Weidemann, "Optical turbulence on underwater image degration in natural environments," Appl. Opt. **51**, 2678-2686 (2012).
[4] W. Hou, E. Jarosz, S. Woods, W. Goode, and A. Weidemann, "Impacts of underwater turbulence on acoustical and optical signals and their linkage," Opt. Express **21**, 4367-4375 (2013).
[5] G. D. Gilbert, and R. C. Honey, "Optical trubulence in the sea," in Underwater Photo-optical Instrumentation Applications **SPIE**, 49-55 (1972).
[6] J. D. Nash, D. R. Caldwell, M. J. Zelman, and J. N. Moum, "A thermocouple probe for high-speed temperature measurement in the ocean," J. Atmos. Ocean Tech. **16**, 1474-1482 (1999).
[7] B. Ward, R. Wanninkhof, P. J. Minnett, and M. J. Head, "SkinDeEP: a profiling instrument for upper-decameter sea surface measurements," J. Atmos. Ocean Tech. **21**, 207-222 (2004).
[8] G. Liu, W. Hou, and M. Han, "High-resolution and fast-response fiber-optic temperature sensor using silicon Fabry-Pérot cavity," Opt. Express **23**, 7237-7247 (2015).
[9] M. N. Özişik, *Heat transfer: a basic approach* (McGraw-Hill, 1985).
[10] W. Qu, G. M. Mala, and D. Li, "Heat transfer for water flow in trapezoidal silicon microchannels," Int. J. Heat Mass Transfer **43**, 3925-3936 (2000).
[11] S. Matt, W. Hou, W. Goode, G. Liu, M. Han, A. Kanaev, and S. Restaino, "A controlled laboratory environment to study EO signal degradation due to underwater turbulence," Proc. SPIE **9459-18** (2015).